

# Numerical Simulation of Thermal and Flow Fields in Induction Skull Melting Process

Xue Guanxia<sup>1</sup>, Wang Tongmin<sup>1</sup>, Su Yanqing<sup>2</sup>, Cai Shaowu<sup>1</sup>, Xu Jingjing<sup>1</sup>,  
Li Jun<sup>1</sup>, Guo Jingjie<sup>2</sup>, Li Tingju<sup>1</sup>

<sup>1</sup>Dalian University of Technology, Dalian 116024, China; <sup>2</sup>Harbin Institute of Technology, Harbin 150001, China

**Abstract:** The electromagnetic, thermal and fluid fields during ISM (Induction Skull Melting) of TiAl alloy are simulated. The effects of ampere-turn, frequency and relative position between crucible and coil on the distribution of thermal and flow fields are numerically studied. The simulation model is verified by experiments and the simulation results are discussed in detail.

**Key words:** ISM; simulation; suspending hump; thermal field; flow field

Induction Skull Melting (ISM) is used to melt high melting point, high purity and very active metals. During ISM, the charge is heated with high frequency magnetic field. After melting, the melt is suspended by the electromagnetic force avoiding to be polluted. Many physical phenomena are involved in ISM, such as induction heating, electromagnetic stirring, electromagnetic suspending etc.<sup>[1]</sup>. Usually We need to spend much time and money on ISM parameter study by experiments.

Simulation work on ISM was started in the middle of 1990s. Most of researchers simulated the simplex temperature field using their own programs<sup>[2]</sup>. Recently, researchers simulate two or more physics fields using commercial simulation soft<sup>[3,4]</sup>. Bojarevics and Pericleous used an axisymmetric pseudo-spectral representation model to solve the thermal and flow fields<sup>[5,6]</sup>. But the model relied on the finite volume and integral equation to represent particular details of the problem. Baake and Umbrashko et al. used commercial software to simulate the process of ISM. They got the optimal degree of superheat, improved total efficiency, induced energy dissipation controlled alloy component and induced skull thickness<sup>[7]</sup>. Song et al. simulated the electromagnetic field, heat transfer and fluid flow in a water cold crucible which was a mixture of UO<sub>2</sub> and ZrO<sub>2</sub><sup>[8]</sup>.

## 1 Simulation Model

Received date: May 10, 2008

Foundation item: National Natural Science Foundation of China (No.505601003); Natural Science Foundation of Liaoning Province (No.20052176); The Project-sponsored by SRF for ROCS, SEM ([2006]331), and Program of New Century Excellent Talents in University (NCET-07-0137)

Biography: XueGuanxia, Master, School of Material Science and Engineering, Dalian University of Technology, Dalian 116024, P. R. China; Corresponding Author: Wang Tongmin, Associate Professor, Tel: 0086-411-84706790, E-mail: tmwang@dlut.edu.cn

Copyright © 2009, Northwest Institute for Nonferrous Metal Research. Published by Elsevier BV. All rights reserved.

The Maxwell equations are solved to get the data of electromagnetic field such as electromagnetic force, magnetic field intensity and Joule heat etc.<sup>[9,10]</sup>. Afterwards, the electromagnetic force is introduced into the momentum equations to consider the effect of electromagnetic stirring. The Joule heat is introduced into the energy equations to consider the effect of induction heat. For the flow within the crucible is a typical turbulent flow, the  $k-\varepsilon$  turbulent flow model is adopted.

The suspending hump in ISM process plays an important role for melting quality. In the view of simulation, the suspending hump is not only the pressure boundary but also the heat radiation boundary. The suspending hump height can be calculated based on the balance of electromagnetic force and metal static pressure. The relationship between magnetic intensity and hump height is expressed as below<sup>[11]</sup>:

$$B = \sqrt{2\mu\rho gh} \quad (1)$$

Where  $B$  is magnetic intensity,  $\mu$  is permeability,  $\rho$  is density,  $g$  is gravity acceleration and  $h$  is hump height.

When the metal melted completely, a layer of skull formed between the metal liquid and skull, so the thermal boundary condition between the metal liquid and skull is mixture boundary condition of radiation and thermal conductivity. It can be expressed as follows:<sup>[3]</sup>

$$q = H_{ch}(T - T_w) \quad (2)$$

Where  $q$  is heat flux,  $T_w$  the wall temperature (in this case fixed to the average temperature of the cooling liquid inside the copper wall),  $H_{ch}$  is an empirical heat transfer coefficient and can be obtained from comparisons with the experimentally measured heat losses at the water-cooled walls. It depends on the metal temperature  $T$  at the wall contact position:

$$\begin{aligned} H_{ch} &= 150 && \text{if } T < T_s \\ H_{ch} &= 150 + (T - T_s) \times 200 && \text{if } T \geq T_s \end{aligned} \quad (3)$$

Where  $T_s$  is metal melting point, and  $T$  is metal temperature at the skull inside wall.

In the surface of suspending hump, the radiation condition is used [8]:

$$q = \varepsilon \sigma_B (T^4 - T_w^4) \quad (4)$$

Where the emissivity  $\varepsilon$  is set to 0.3 and  $\sigma_B$  is Stefan-Boltzman constant.

### 2 Simulation Procedure and Experiment Validation

It is assumed that: (1) The magnetic field is harmonic. (2) The flow is incompressible flow. (3) The suspending hump is supposed to be paraboloid. (4) The simulation starts from the moment of hump formation.

The geometry and enmeshed models are shown in Fig.1. The charge is Ti6Al4V, whose property parameters are widely known. The electromagnetic field was solved using ANSYS<sup>TM</sup>. The simulated Lorenz force and Joule heat are shown in Fig.2 and Fig.3, respectively. The momentum and energy equations were solved using FLUENT<sup>TM</sup>. In order to consider the electromagnetic effects in thermal and flow calculations, the Lorenz force and Joule heat were transferred from ANSYS<sup>TM</sup> to FLUENT<sup>TM</sup> by a special-user-defined subroutine coded by C language.

An experiment was done for verifying the simulation model. The molten melt was poured into a mould (232 mm×232 mm×58 mm) which was surrounded by a five-turn coil supporting a 777 Hz and 4036 ampere-turn alternative current. The magnetic intensity at the predefined line was measured and compared with the simulation result obtained under the same conditions. Basically, the simulated results are consistent with the experimental results as shown in Fig.4. The simulated suspending hump is also compared with that from experiment. The good agreement is obtained for both shape and height of the suspending hump as shown in Fig.5 and Fig.6.

### 3 Results and Discussion

#### 3.1 Suspending hump analysis

Fig.7 shows the influence of the input ampere-turn on the hump height. The hump height increases with increasing of ampere-turn. Averagely the height of the suspending hump increases by 4 mm per 1000 ampere-turn increment

Fig.8 shows the influence of the relative position between crucible and coil on the hump height. The relative position denoted by  $h$  means the distance from the bottom coil to the

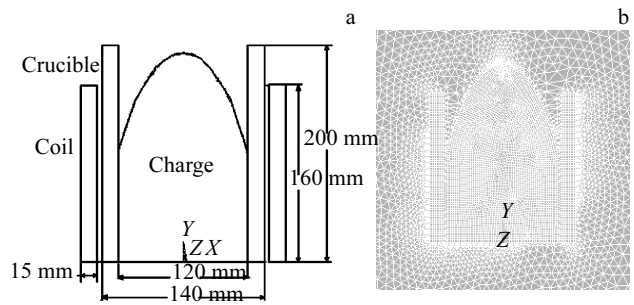


Fig.1 Geometry (a) and enmeshed models (b)

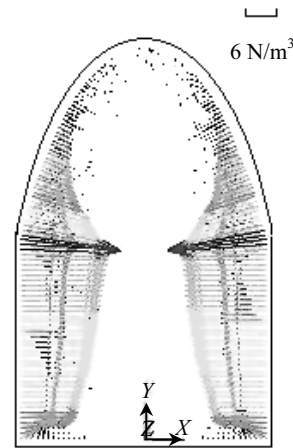


Fig.2 Lorenz force distribution

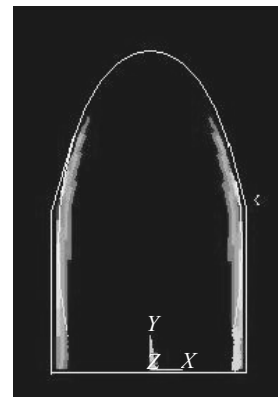


Fig.3 Joule heat distribution

bottom of the crucible. It is noted that the hump height increases with decreasing of the relative position. The hump height has a jump increase when the relative position is approaching zero.

#### 3.2 Thermal field analysis

Fig.9 shows the change of the maximal temperature of molten metal with different ampere-turn when the melting time is 211 s. It is noted that the relation between the maximal temperature and ampere-turn is almost linear. Averagely, the

maximal temperature increases by 20 K per 1000 ampere-turn increment.

Fig.10 shows the temperature distribution of molten metal ( $t=451$  s), and Fig.11 shows the temperature distribution at A-A cross section. It can be seen from the both figures that the temperature difference inside the molten melt is very small. The maximum difference is less than 5 K.

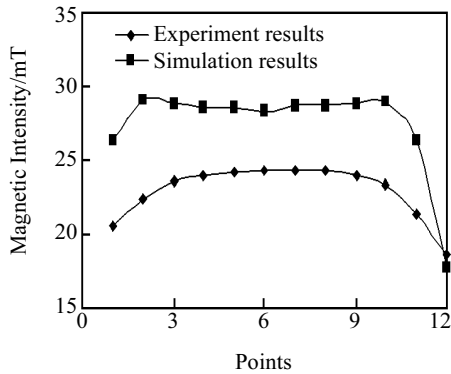


Fig.4 Comparison between experiment results and simulation results

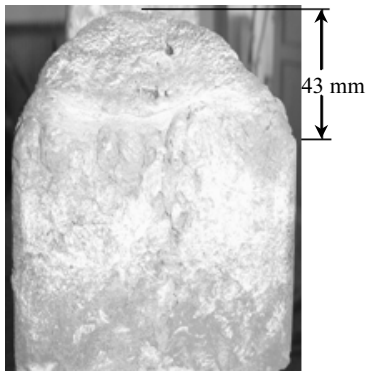


Fig.5 Side view of ingot

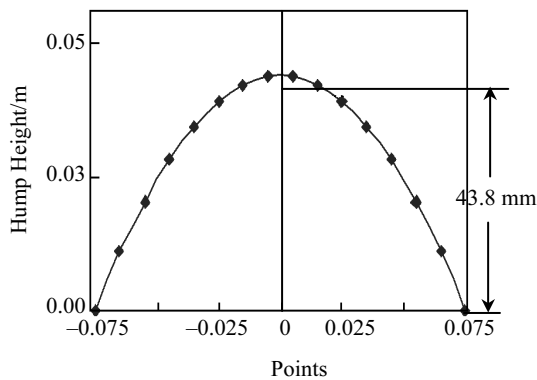


Fig.6 Simulated suspending hump

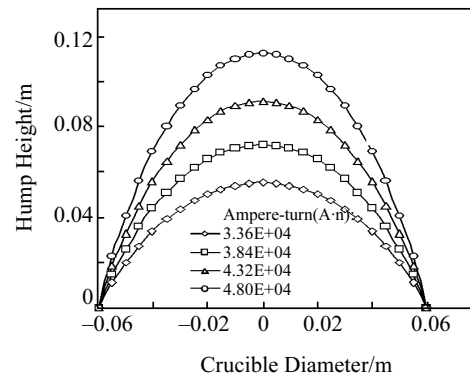


Fig.7 Influence of ampere-turn on suspending hump

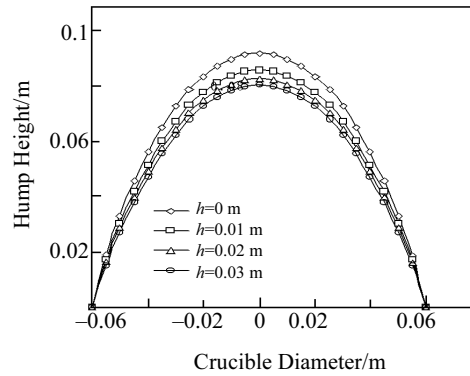


Fig.8 Influence of the relative position between crucible and coil on the suspending hump

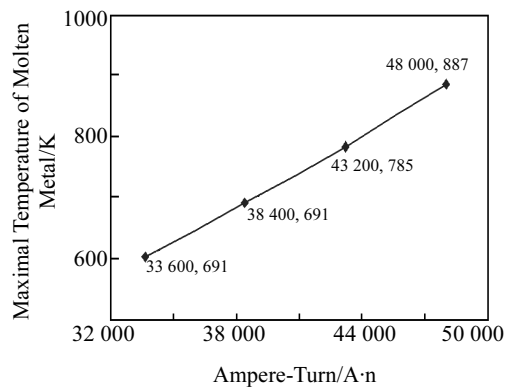


Fig.9 The change of the maximal temperature of molten metal with different ampere-turn ( $t=211$ s)

Fig.12 shows the change of the maximal temperatures of the molten metal with different frequencies when the melting time is 211 s. It is noted that the maximal temperature increases with increasing of frequency (200 K/1000 Hz) before 5000 Hz and the maximal temperature increases slightly after 5000 Hz.

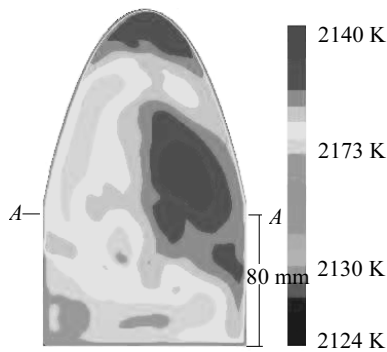


Fig.10 The temperature distribution of molten metal ( $t=45$ s the end of melting)

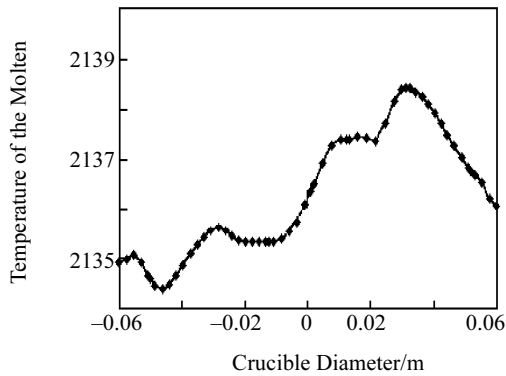


Fig.11 The temperature distribution at A-A cross section

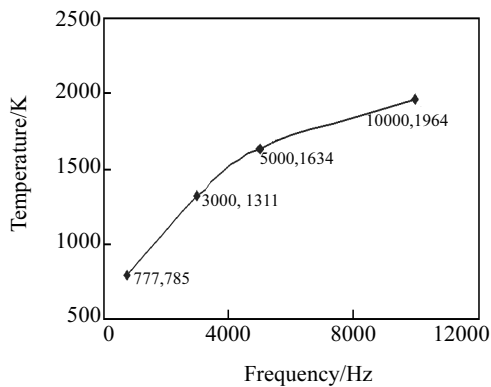


Fig.12 Influence of the frequency on thermal field when  $t=211$ s

### 3.3 Flow field analysis

There are three typical flow patterns as shown in Fig.13. The flows start from the area near the crucible towards the center forming two or more turbulent swirls. The swirls dynamically change with the increase of the melting time due to the dynamic balance of the two flow streams coming from two sides of the crucible.

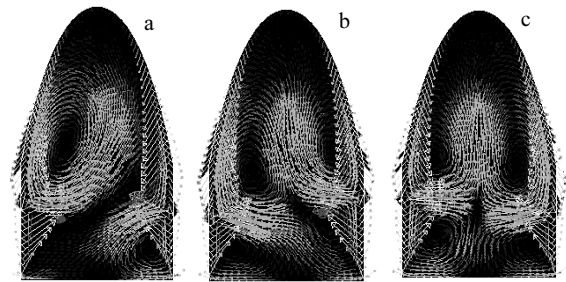


Fig.13 Three typical flow patterns during ISM: (a) flow pattern 1, (b) flow pattern 2, and (c) flow pattern 3

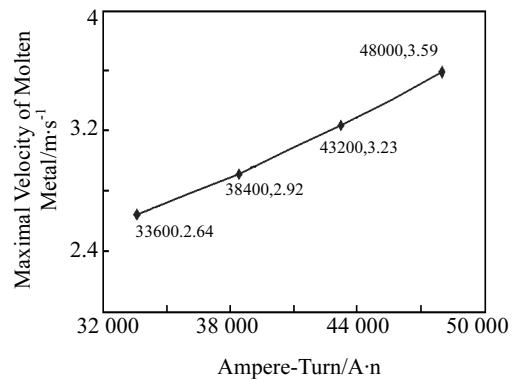


Fig.14 Influence of ampere-turn on the maximal fluid velocity

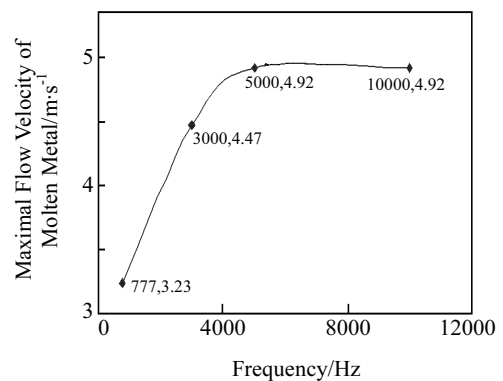


Fig.15 Influence of frequency on the maximal flow velocity

As can be seen in Fig.14, the maximal fluid velocity of the molten metal increases approximately with the increase of ampere-turn. The maximal fluid velocity increases by about 0.075 m/s per 1000 ampere-turn increment

It can be seen from Fig.15 that the maximal fluid velocity increases with the increase of frequency before 3000 Hz, i.e. increases by about 0.4 m/s per 1000 Hz increment. But there is no obvious increment after 3000 Hz.

## 4 Conclusion

1) The simulation method for ISM process including the treatments of suspending hump, induction heating and elec-

tromagnetic stirring can be realized. It is in good agreement with experimental results.

2) For the present simulation study, the hump height increases by 4.2 mm. the maximal temperature increases by 20 K; the maximal fluid velocity increases by 0.075 m/s per 1000 ampere-turn increment.

3) For the present simulation study, the maximal temperature increases by 200 K per 1000Hz increment before 5000 Hz but has no distinct increment after 5000 Hz; the maximal fluid velocity increases by 0.4 m/s per 1000 Hz increment before 3000 Hz but has no distinct increment after 3000 Hz.

## References

- 1 Su Yanqing(苏彦庆), Ren Zhijiang (仁志江), Guo Jingjie(郭景杰). *Material Science and Technology*(材料科学与工艺)[J], 1999, 7(2): 39
- 2 Wang Tongmin(王同敏). *Numerical Simulation of the Temperature Fields in Cold Wall Induction Melting Process of Special Alloy*(特种合金在冷壁感应熔炼过程的温度场数值模拟研究)[D]. Harbin: Harbin Institute of Technology, 1997
- 3 Zhang Yongjie(张永杰), Deng Anyuan(邓安元). *Computers and Applied Chemistry*(计算机应用化学)[J], 2006, 7
- 4 Zhang Xingguo(张兴国), Qu ruojia(曲若家). *Special Casting & Nonferrous Alloys*(特种铸造及有色合金)[J], 2004, 6: 12
- 5 Bojarevics V, Harding R A, Pericleous K. *Metallurgical and Materials Transactions B*[J], 2004, 35B(4):785
- 6 Bojarevics V, Pericleous K. *Journal of Materials Science*[J], 2004, 39(24): 7245
- 7 Baake E, Umbrashko A, Jakovics A. *LES modeling of the Cold Crucible Melting Process*[C]. Dresden: The 2nd Sino-German Workshop on EPM, 2005
- 8 Song J H, Min B T, Kim J H et al. *International Communications in Heat and Mass Transfer*[J], 2005, 32(10): 1325
- 9 Zhu Shoujun(朱守军), Deng Fei(邓飞), Tu Guanzhen(屠关镇). *Industry Heating*(工业加热)[J], 1996, 1: 11
- 10 Zhang Jun(张军), Fu Hengzhi (付恒志). *Material Research Transaction*(材料研究学报)[J], 1997, 11(6):612
- 11 Jia Fei(贾非). *Optimization of Technical and Study of Structure Property for Electromagnetic Continuous Casting*(电磁连续铸造过程工艺优化及组织性能研究)[D]. Dalian: Dalian University of Technology, 2002: 29

## 感应凝壳熔炼过程热与流场耦合数值模拟研究

薛冠霞<sup>1</sup>, 王同敏<sup>1</sup>, 苏彦庆<sup>2</sup>, 蔡少武<sup>1</sup>, 许菁菁<sup>1</sup>, 李军<sup>1</sup>, 郭景杰<sup>2</sup>, 李廷举<sup>1</sup>

(1. 大连理工大学, 辽宁 大连 116024)

(2. 哈尔滨工业大学, 黑龙江 哈尔滨 150001)

**摘要:** 模拟研究了 TiAl 合金感应凝壳熔炼过程的热场和流场分布, 探讨了安培匝、电源频率以及坩埚与感应线圈的相对位置等电磁参数对热及流场分布的影响规律, 模拟模型通过实验测得的磁感强度以及搅拌驼峰高度进行了有效验证, 并对模拟结果进行了详细的分析讨论。

**关键词:** 感应凝壳熔炼; 模拟; 搅拌驼峰; 热场; 流场

---

作者简介: 薛冠霞, 女, 1983年生, 硕士, 大连理工大学材料科学与工程学院, 辽宁 大连 116024; 通讯作者: 王同敏, 副教授, 电话: 0411-84706790, E-mail: tmwang@dlut.edu.cn